

The rotation of pentaphenylphenyl groups and their terminal phenyl groups: a variable-temperature ^1H NMR study on an albatrossene and a three-bladed molecular propeller

Hartmut Komber,* Katrin Stumpe and Brigitte Voit

Leibniz Institute of Polymer Research, Hohe Strasse 6, 01069 Dresden, Germany

Received 24 January 2007; revised 14 February 2007; accepted 16 February 2007

Available online 20 February 2007

Abstract—Dynamic NMR of 1-phenylethynyl-3,5-bis(pentaphenylphenyl)benzene (**1**) and 1,3,5-tris(pentaphenylphenyl)benzene (**2**) allows us to determine two rotational barriers for each compound. For **1**, a first process exhibits $\Delta G^\ddagger = 39.2$ kJ/mol followed by a second one with a ΔG^\ddagger value of 69.9 kJ/mol. Two processes with similar rotational barriers are found for **2** (70.9 and 75.3 kJ/mol). Motional processes which can be related to these barriers are 60° and 180° rotations of the pentaphenylphenyl units about the single bond with the core benzene ring and rotation of the terminal phenyl rings of the pentaphenylphenyl units. The results are discussed considering the consequences of these processes on the NMR spectra.
© 2007 Elsevier Ltd. All rights reserved.

Much effort was devoted to the development of synthetic routes towards polyphenylene dendrimers with increasing generations and different substituents over the last decade, and thus a multitude of such dendrimers has been reported.^{1–3} The all-phenylene scaffold is characterized by a high stiffness. This rigidification is linked with an increasing shape persistence of these polyphenylenes which can reach nanometer dimensions depending on the generation realized.⁴ The size and the shape in combination with a sophisticated chemical structure offer a variety of applications in the field of nanomaterials.^{1,2}

A close inspection of these dendrimer structures shows that they are formed by a low number of characteristic subunits; 1,3,5-triaryl-, pentaaryl- and hexaarylbenzenes are most commonly found. This also applies for the less regular hyperbranched polyphenylenes.⁵ A well proven way to gain access to large and complex structures is the study of smaller substructures. Following this approach, we have recently analyzed the NMR spectra of hyperbranched polyphenylenes. In the course of that study, oligophenylenes **1** and **2** (Fig. 1) were prepared as

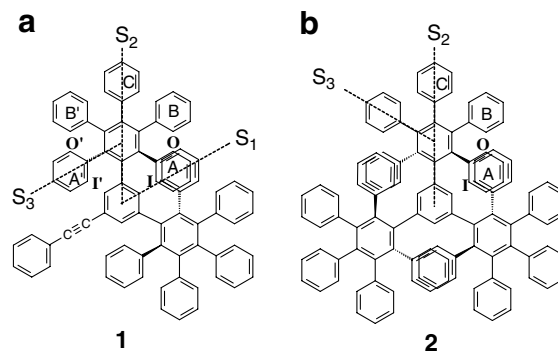


Figure 1. Structures of (a) the albatrossene **1** and (b) three-bladed molecular propeller **2** with some rotational axes and assignments for terminal rings and *ortho*-protons of rings A and A'.

model compounds of the substructures and characterized by ^1H and ^{13}C NMR spectroscopy.⁶

These compounds are based on an 1,3,5-trisubstituted benzene core and show structural motifs also referred to as albatrossene⁷ (**1**) and three-bladed molecular propeller (**2**).

Similar compounds with further increased packing density by additional phenyl or polyphenylene substitution in the 2-, 4- and 6-position of the central benzene ring were published recently.^{8–10}

Keywords: Conformational analysis; Dynamic NMR; Polyphenylenes; Oligophenylenes.

* Corresponding author. Tel.: +49 351 4658343; fax: +49 351 4658565; e-mail: komber@ipfdd.de

The understanding of molecular dynamics in polyphenylenes is of fundamental interest.¹¹ With success in synthesizing large-size polyphenylenes the dynamics of bulky polyphenylene subunits both in solid and solution gain increasing importance. Solid-state NMR investigations of a series of polyphenylene dendrimers using different techniques allowed the elucidation of slow as well as of fast dynamics.¹² Intramolecular steric constraints dominate the molecular dynamics which are characterized by fast vibrations of terminal phenyl rings and slow two-site jumps of terminal and *para*-substituted phenyl rings with a mean reorientation angle of 24° of term, presumably in a concerted process involving several adjacent rings. However, the dendrons cannot reorient even at high temperatures.

The small-sized dendrimers **1** and **2** are predestined for a dynamic study in solution because their spectra are not too complex for a complete signal assignment and they are sufficiently soluble also at low temperatures. Furthermore, the rotational behaviour of their phenyl rings or whole pentaphenylphenyl moieties is not influenced by substituents. In order to explain the dynamic processes observed by NMR for hyperbranched polyphenylenes in solution we came up with preliminary results of such a study.⁶ Here we give a more detailed analysis of the solution-state dynamics of bulky pentaphenylphenyl moieties and their terminal phenyl groups studied by variable-temperature ¹H NMR.

The X-ray structure of **2**⁷ and the calculated molecular structure of **1** (Fig. 2),¹³ whose typical features are in accordance with the crystal structures of 1,3-bis(pentaphenylphenyl)benzene⁹ and a derivative of **1** with additional phenyl groups in 2-, 4- and 6-position,¹¹ reveal interlocking phenyl rings resulting in steric constraints. These structures also suggest that different phenyl rings within the pentaphenylphenyl moieties in **1** and **2** can be distinguished and, in addition, all in all four different *ortho*-protons for rings A and A' of **1** (Figs. 1 and 2) and two different *ortho*-protons for ring A of **2** (Fig. 1). We will return to this point later with respect to the interpretation of the NMR results.

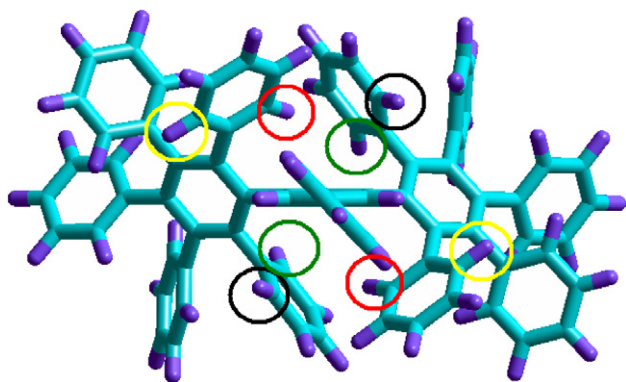


Figure 2. Molecular modelling drawing of **1** (S_1 direction) showing the *ortho*-protons of rings A and A' located in the shielding region of a nearby aromatic ring (I; red circles), nearby the 4-proton of the 1,3,5-trisubstituted benzene (I', green circles) and the other *ortho*-protons of rings A and A' (O, O'; yellow and black circles, respectively).

First hints to restricted rotations in **1** and **2** were obtained from their room temperature (rt) ¹³C NMR spectra which show more signals than expected in the fast exchange limit for all single-bond rotations (28 vs 26 for **1** and 21 vs 18 for **2**).⁶ EXSY spectra confirmed the occurrence of exchange slow on the ¹H NMR time scale at rt for both compounds and pointed out the crucial importance of a high-field shifted doublet occurring in both ¹H NMR spectra (at 6.18 ppm for **1** and 5.72 ppm for **2**, CDCl₃, 300 K) for the understanding of the dynamic processes (see [Supplementary data](#)). Such high-field shifted signals were reported also for other structurally similar polyphenylenes and were attributed to protons which are located in the shielding region of nearby aromatic rings.^{7,8,10} In fact, the X-ray structure of **2**⁷ reveals that one *ortho*-proton of each ring A (I in Fig. 1b) is positioned near the face of an A-ring of the neighboring pentaphenylphenyl ring (edge-to-face orientation of these rings). Six protons of this type are in accordance with the integral ¹H NMR intensity of this signal. X-ray structures of 1,3-bis(heptaphenyl-2-naphthyl)benzenes⁷ and 1,3-bis(pentaphenylphenyl)benzenes^{10,14} which are structurally similar to **1** and our own results of molecular modelling on **1** (Fig. 2) suggest that *one* proton of each ring A (I in Fig. 1a) but none of A' is located similarly. In contrast, however, the integral ¹H NMR intensity of the high-field signal of **1** represents four instead of the expected two protons.

This apparent discrepancy is clarified by low-temperature measurements in CD₂Cl₂. The lower traces in Figure 3a clearly show a complex decoalescence behaviour at lowest temperatures ending with a total of four non-equivalent *ortho*-protons for the A and A' rings with three of them having chemical shifts similar to those of the rings B, B' and C (Fig. 3b). Each signal represents two protons as expected. It is remarkable that the chemical shift of the new high-field signal (5.18 ppm) is comparable to that of **2** at the same temperature (5.30 ppm, 186 K). Because position I in both compounds is characterized by interlocking *ortho*-phenyl groups of pentaphenylphenyl blades or wings, a similar surrounding is suggested by the structures and confirmed by the NMR data. Note that no high-field shifted signal is observed for the derivative with one pentaphenylphenyl and two phenylethynyl groups.⁶ The signals of the phenylethynyl group also remain nearly unchanged at the lowest temperature indicating fast rotation. Probably due to the bulkiness of the wings there is no indication of a diastereomer with one pentaphenylphenyl unit that has a torsion angle about S_2 , which is of opposite sign with respect to that of the other unit.

Extending the temperature range by high-temperature measurements using CDCl₂CDCl₂ as solvent, a second coalescence process is observed (upper traces in Fig. 3a). The two-step coalescence observed over the full temperature range (Fig. 3a and b) indicates at least two dynamic processes. Their activation parameters were estimated at the coalescence temperatures as outlined in [Supplementary data](#). We rationalize the first signal coalescence with an uncorrelated 60° rotation of both wings about the S_2 axes resulting in the enantiomeric

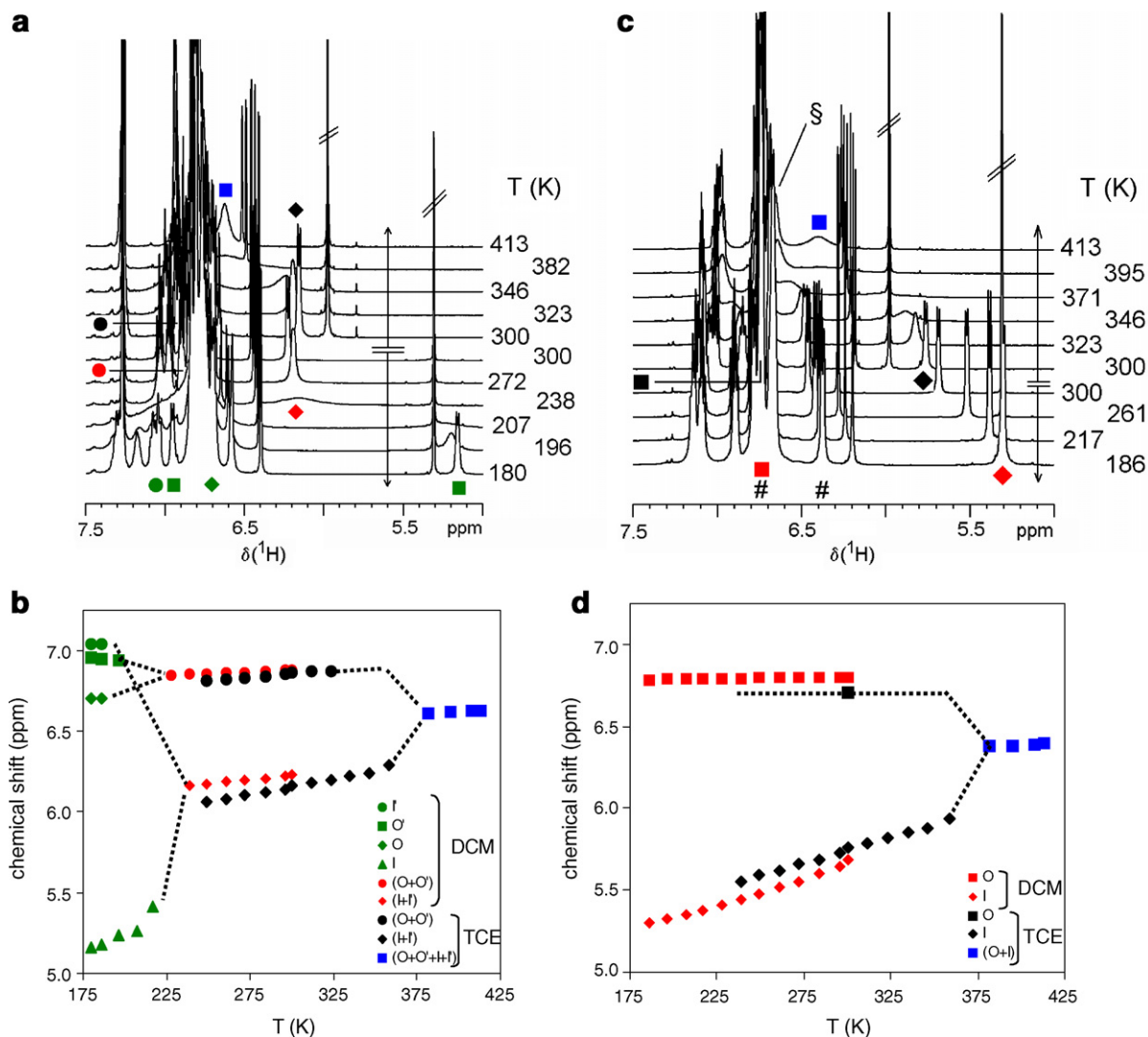


Figure 3. Selected variable-temperature (VT) ^1H NMR spectra of (a) **1** and (c) **2**. The spectra of the lower part ($T \leq 300$ K) were measured in CD_2Cl_2 (DCM) and the spectra of the upper part ($T \geq 300$ K) in $\text{CDCl}_2\text{CDCl}_2$ (TCE). The symbol # indicates the two *ortho*-proton signals of ring B of **2** at slow exchange and the signal at fast exchange is indicated by §. The other symbols correspond with the graphs showing the experimentally determined temperature dependency of the *ortho*-proton signals of (b) rings A and A' of **1** and (d) rings A of **2**. Dotted lines mark temperature regions in which the chemical shifts could not be determined because of signal overlap or signal broadening. In addition, they connect signals in the slow and fast exchange region.

form and in the following signal coalescences: $\text{I} = \text{I}'$ and $\text{O} = \text{O}'$. A careful inspection of the EXSY/ROESY spectrum of **1** at 183 K shows that the proton which exchanges with proton I is really proton I' (comp. Fig. 2), which can be identified by its ROESY cross-peak to the nearby proton in 4-position of the 1,3,5-trisubstituted benzene ring (see Supplementary data). The activation barrier of this 60° rotation was found to be 39.2 kJ/mol ($k_c = 2$ kHz at 219 K).

The second process slow at 300 K but rapid at $T > 375$ K (Fig. 3a and b) results in time-averaging of all four *ortho*-protons ($\text{I}/\text{I}' = \text{O}/\text{O}'$). The estimated ΔG^\ddagger for this process is 69.9 kJ/mol ($k_c = 200$ Hz at 346 K). With the fast 60° rotation, several processes can result in this signal coalescence: uncorrelated 180° rotation of one wing or correlated 180° rotation of both wings and fast rotation of the *ortho*-phenyl rings A and

A' about the S_3 axis. For the latter process, Gust et al. determined rotation barriers of ~ 70 kJ/mol for substituted terminal phenyl rings of hexaphenylbenzenes.¹⁵ Pascal et al. have shown that the barrier for the uncorrelated 180° rotation of the blades is ~ 79 kJ/mol for a desymmetrized hexamethoxy derivative of **2**.⁷ This barrier should be lower for **1** due to lower steric constraints caused by two pentaphenylphenyl substituents only. Concluding, we are not able to distinguish unambiguously between these three processes by ΔG_c^\ddagger and it is not impossible that all of these processes are of comparable energy.

Excepting the correlated 180° rotations of three interlocking blades,¹⁶ the processes discussed for **1** can also occur for **2**, but their consequences on the NMR spectrum of the more symmetric **2** are different. Slow uncorrelated 180° rotation about S_2 cannot be directly

observed in D_3 symmetric **2** but both the slow 60° rotation about S_2 and the slow phenyl ring rotation about S_3 would result in the same effect: nonequivalence of *ortho*-protons I and O (Fig. 1). No decoalescence process could be observed in the low temperature experiment and the nonequivalence of *ortho*-protons I and O indicates that both the 60° rotations of the blades and the terminal phenyl ring rotations are in the slow rotation regime over a wide temperature range (Fig. 3c and d). The high field shift with decreasing temperature observed for the signal of protons I indicates a compaction of the molecule, for example, by lower vibrational motion. Similar chemical shifts for protons I were observed for **1** and **2** below ~ 225 K (Fig. 3) confirming that at this temperatures the blades of both compounds are in the same slow rotation regime. Even though one expects a higher rotation barrier for rotations about S_2 in **2** compared to **1** because of more intense interlocking of the three pentaphenylphenyl blades, the stiffness of **2** is remarkable because of the relative low barrier found for the 60° rotation in **1**.

From the number of signals, the presence of an additional diastereomeric false-propeller conformer in which one pentaphenylphenyl unit has a torsion angle about S_2 , which is of opposite sign with respect to that of the other units was not proven.

The high temperature behaviour of **2** (upper part of Fig. 3c and d) is similar to that of **1**. Signal coalescence is observed for signals of phenyl rings A and B (Fig. 4) and the rotation rates and activation parameters were estimated at the coalescence temperatures to be $\Delta G^\ddagger = 70.9$ kJ/mol ($k_c = 224$ Hz at 352 K) for ring A signals and $\Delta G^\ddagger = 75.3$ kJ/mol ($k_c = 242$ Hz at 374 K) for ring B signals. As mentioned above, two processes can result in equivalence of pairs of ‘inner’ and ‘outer’ protons of terminal phenyl rings of **2**: concerted 60° rotation of the three blades about the S_2 axes and fast rotation about the S_3 axes. The first process involves all terminal phenyl rings and would result in the same ΔG^\ddagger value for rings A and B. However, the difference

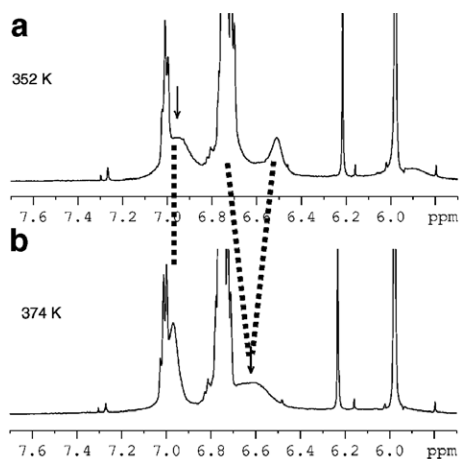


Figure 4. Signal coalescence of (a) *meta*-protons of ring A ($\Delta G^\ddagger = 70.9$ kJ/mol) and (b) *ortho*-protons of ring B ($\Delta G^\ddagger = 75.3$ kJ/mol). Note that the B-ring signals are still separated at 352 K.

of 4.4 kJ/mol measured in the same experiment points to different motions causing these barriers. The first barrier obviously belongs to the rotation of phenyl rings A about S_2 , whereas the second motion could be the concerted 60° rotation of all three blades or the rotation of phenyl rings B about S_2 .

In summary, rotation rates and activation parameters were determined from VT ^1H NMR spectra of **1** and **2** extending the very limited number of activation parameters available for such bulky polyphenylenes. The motional processes could be rationalized as rotations of the bulky pentaphenylphenyl groups and/or of their terminal phenyl groups. However, the complex dynamic behaviour of these compounds prevented an unambiguous correlation between observed signal coalescence processes and rotation processes in two cases. Studies on the conformational equilibria of polyphenylenes by computational methods should provide an additional insight concerning the barriers of the different motions.

^1H NMR spectra (500 MHz) were recorded on a Bruker Avance 500 spectrometer. The spectra were referenced on residual solvent protons signals. Low temperature experiments were carried out in CD_2Cl_2 ($\delta(^1\text{H}) = 5.31$ ppm), whereas $\text{CDCl}_2\text{CDCl}_2$ was used as solvent for high temperature measurements ($\delta(^1\text{H}) = 5.98$ ppm). The temperature was controlled by the Bruker variable temperature accessory BVT 3000 and was calibrated using the standard Wilmad methanol and ethylene glycol samples. The temperature remained stable better than ± 0.5 °C during the experiments.

Compounds **1** and **2** were synthesized from 1,3,5-tris(phenyletynyl)benzene and tetraphenylcyclopentadienone using a 1:2.2 and 1:3.3 molar ratio, respectively. The syntheses were performed under argon atmosphere at 230 °C in diphenylether employing an educt concentration of 0.3 mol/L. The reaction time varied from 120 h for compound **1** to 380 h for compound **2**. The products were recovered by precipitation into ethanol, filtered and washed with methanol. Purification was done by precipitation from chloroform with ethanol. Melting points: **1**: 357 °C (determined by DSC) and **2**: 242 °C (lit.: 242 – 244 °C).⁷

Acknowledgement

The authors thank Professor R. Pascal, Jr. for valuable suggestions and discussions.

Supplementary data

More experimental details, syntheses of **1** and **2**, NMR data including 1D and 2D spectra, extended sets of VT ^1H NMR spectra, the calculations of k_c and ΔG_c^\ddagger values and further molecular modelling drawings for **1** and **2** are given. Supplementary data associated with this article can be found, in the online version, at doi:10.1016/j.tetlet.2007.02.079.

References and notes

1. (a) Berresheim, A. J.; Müller, M.; Müllen, K. *Chem. Rev.* **1999**, *99*, 1747–1785; (b) Wiesler, U.-M.; Weil, T.; Müllen, K. *Top. Curr. Chem.* **2001**, *212*, 1–40; (c) Bauer, R. E.; Grimsdale, A. C.; Müllen, K. *Top. Curr. Chem.* **2005**, *245*, 253–286.
2. Grimsdale, A. C.; Müllen, K. *Angew. Chem., Int. Ed.* **2005**, *44*, 5592–5629.
3. Pascal, R. A., Jr. *Chem. Rev.* **2006**, *106*, 4809–4819.
4. Andreitchenko, E. V.; Clark, C. G., Jr.; Bauer, R. E.; Lieser, G.; Müllen, K. *Angew. Chem., Int. Ed.* **2005**, *44*, 6348–6354.
5. (a) Kim, Y. H.; Webster, O. W. *Macromolecules* **1992**, *25*, 5561–5572; (b) Morgenroth, F.; Müllen, K. *Tetrahedron* **1997**, *53*, 15349–15366; (c) Häußler, M.; Lam, J. W. Y.; Zheng, R.; Peng, H.; Luo, J.; Chen, J.; Law, C. C. W.; Tang, B. Z. *C. R. Chimie* **2003**, *6*, 833–842; (d) Stumpe, K.; Voit, B.; Komber, H. *Macromol. Chem. Phys.* **2006**, *207*, 1825–1833.
6. Komber, H.; Stumpe, K.; Voit, B. *Macromol. Chem. Phys.* **2006**, *207*, 1814–1824.
7. Tong, L.; Ho, D. M.; Vogelaar, N. J.; Schutt, C. E.; Pascal, R. A., Jr. *J. Am. Chem. Soc.* **1997**, *119*, 7291–7302.
8. Bauer, R. E.; Enkelmann, V.; Wiesler, U. M.; Berresheim, A. J.; Müllen, K. *Chem. Eur. J.* **2002**, *8*, 3858–3864.
9. Shen, X.; Ho, D. M.; Pascal, R. A., Jr. *J. Am. Chem. Soc.* **2004**, *126*, 5798–5805.
10. Wasserfallen, D.; Matternsteig, G.; Enkelmann, V.; Müllen, K. *Tetrahedron* **2006**, *62*, 5417–5420.
11. Brydges, A.; Harrington, L. E.; McGlinchey, M. L. *Coord. Chem. Rev.* **2002**, *233–234*, 75–105.
12. Wind, M.; Saalwächter, K.; Wiesler, U.-M.; Müllen, K.; Spiess, H. E. *Macromolecules* **2002**, *35*, 10071–10086.
13. All attempts to prepare crystals for an X-ray study failed. The molecular models were obtained using the HyperChem™ 7.5 software package from Hypercube Inc. The MM+ molecular mechanics force field implemented in this software was applied in geometry optimization using the Polak–Ribiere algorithm. The molecules were calculated in vacuum.
14. Müller, M.; Iyer, V. S.; Kübel, C.; Enkelmann, V.; Müllen, K. *Angew. Chem., Int. Ed.* **1997**, *36*, 1607–1610.
15. (a) Gust, D. *J. Am. Chem. Soc.* **1977**, *99*, 6980–6982; (b) Gust, D.; Patton, A. *J. Am. Chem. Soc.* **1978**, *100*, 8175–8181; (c) Patton, A.; Dirks, J. W.; Gust, D. *J. Org. Chem.* **1979**, *44*, 4749–4752.
16. Chance, J. M.; Geiger, J. H.; Okamoto, Y.; Aburatani, R.; Mislow, K. *J. Am. Chem. Soc.* **1990**, *112*, 3540–3547.